American Society of Mechanical Engineers

ASME Accepted Manuscript Repository

Institutional Repository Cover Sheet

	First	*Last*

ASME Paper Title: Electro-Osmotic Propulsion of Jeffrey Fluid in a Ciliated Channel Under the Effect of Nonlinear Rad and Heat Source/Sink

Authors: Sidra Shaheen , OA Beg , Farah Gul , Khadija Maqbool

ASME Journal Title: Journal of Biomechanical Engineering

Volume/Issue ___Vol. 143, Issue 5_____ Date of Publication (VOR* Online) 4th March 2021

ASME Digital Collection URL: https://asmedigitalcollection.asme.org/biomechanical/article-abstract/doi/10.1115/1.4049810/1096600/Electro-Osmotic-Propulsion-of-Jeffrey-Fluida?redirectedFrom=fulltext

DOI: https://doi.org/10.1115/1.4049744

*VOR (version of record)

Electro-osmotic propulsion of Jeffrey fluid in a ciliated channel under the effect of nonlinear radiation and heat source/sink

S. Shaheen[1], O. Anwar Bég[2], F.Gul[1], K. Maqbool[1*]

[1] *Department of Mathematics & Statistics, International Islamic University, Islamabad 44000, **Pakistan**.*
[2] *Department of Mechanical and Aeronautical Engineering, Salford University, Salford M54WT, England, **UK**.*

Abstract:
Mathematical modelling of mechanical system in microfluidics is an emerging area of interest in micro scale engineering. Since microfluidic devices use the hair like structure of artificial cilia for pumping, mixing and sensing in different fields, therefore; electro osmotic cilia driven flow help to generate the fluid velocity for the Newtonian and viscoelastic fluid. Due to the deployment of artificial ciliated walls, the present research reports the combined effect of an electro osmotic flow and convective heat transfer on Jeffrey viscoelastic electrolytic fluid flow in a two-dimensional ciliated vertical channel. Heat generation/absorption and nonlinear radiation effects are included in the present mathematical model. After applying Debye-Huckel approximation and small Reynolds number approximation to momentum and energy equation, the system of nonlinear partial differential equation is reduced into non-homogenous boundary value problem. The problem determines the velocity, pressure and temperature profiles by the application of semi-analytical technique known as Homotopy Perturbation Method (**HPM**) with the help of software **Mathematica**. The graphical results of the study suggest that **HPM** is a reliable methodology for thermo physical electro-osmotic rheological transport in micro channels.

1 Introduction

Electro-kinetic flows are regarded as electrolytes which are prepared by electrical fields in ducts that have charged walls [1]. A special class of electro-kinetic flow is electro-osmotic flow where the electrostatic body force is large in the electrical double layers and simultaneously the vicinity of the charged no-slip surface leads to significant friction. Electro-osmotic flow is therefore tempted by an applied potential or electric field in a system that has an imbalance of charge. This mechanism is a very efficient technique to create fluid flow in bulk across a charged boundary. It helps to control the flow for proper working in small straits and channels like lab-on-a-chip devices, micro channels, or other fluid conduits. Many practical applications feature such flows including isoelectric protein focusing [2], electrode array design [3], articular cartilage solute transport [4], electro kinetic flow across elliptic cylinder [5] and micro channel [6]. Electro-osmotic flows arise naturally (e.g. in blood flows) and can also be induced artificially in a variety

Corresponding author: Khadija Maqbool, Tel.: +92-51-9019393, E-mail: khadija.maqbool@iiu.edu.pk

of energy and chemical processes. The Debye–Hückel linear approximation is also frequently employed in electro-osmotic flows (EOFs) since it retains some of its physics but greatly simplifies computations. In a study, Marcos *et al.* [7] used a control volume integration method, and staggered grid system to simulate steady state developing electro-osmotic flow in closed-end cylindrical micro-channels. Similarly, Tripathi *et al.* [8] used Mathematica software integration routines to compute the effects of inverse Debye length and Helmholtz–Smoluchowski velocity on micro-capillary peristaltic blood flows. Engineers and applied mathematicians have therefore studied in detail rheological electro-osmotic transport in microsystems with a variety of non-Newtonian constitutive models. Some useful researches in this regard include viscoplastic Casson fluids [9], three-constant Ellis power-law model [10] and Carreau model [11]. All these studies confirmed the substantial deviation from Newtonian behaviour which arises due to various non-Newtonian effects. A simple model is a *Jeffreys elastico-viscous model* [12] which accurately simulates many biophysical fluids and features three constants i.e. viscosity at zero shear rate, and two time-related material parameter constants (for stress relaxation and retardation time).

Cilia are antenna-like membrane-associated structures which exist in many organisms to move the cells or fluid surrounded by it. They exist in arrays on the surface of cells and beat in a coordinated way to clean airways, pass ovum to the uterus, release semen, control embryonic fluid flow etc. as described in [13]-[16]. In recent studies of engineered cilia for bionic microfluidics include Toonder *et al.* [17] (for active micro-fluidic mixing), Balazs *et al.* [18] (for control of particle–surface interactions in micro-bioreactors) and Chateau *et al.* [19] (for hydrodynamic multi-phase flow control). Non-Newtonian ciliated metachronal propulsion has also been examined by a variety of investigators. Manzoor *et al.* [20] used the Blake elliptic cilia model to study magnetohydrodynamic metachronal slip flow of Johnson-Segalman fluids in a channel. They derived perturbation solutions and showed that with greater viscous force relative to elastic force (i.e. smaller Weissenberg viscoelastic number) and increasing cilia length, a substantially larger pressure gradient is needed to sustain the same flux through a narrow region compared with a wider channel.

Jeffrey's visocleastic model has also been deployed in ciliated channel. Relevant studies in recent years include Manzoor *et al.* [21] (who considered porous medium drag effects). Maqbool *et al.* [22] investigated the hydromagnetic ciliary propulsion of Jeffrey viscoelastic fluid in a tilted conduit showing that increasing inclination, magnetic field and cilia length enhances pressure

gradient whereas greater viscoelasticity reduces it.

Another important aspect of modern bio-microfluidics is *heat transfer*. This is important in both natural systems and in manufactured devices. Mercke [23] investigated the air humidity effects in muco-ciliary transport showing that an increase in temperature modifies the ciliary beat frequency. Prodromou *et al.* [24] have shown that thermal shock results in rapid reabsorption in primary cilia in the human body. Mills *et al.* [25] have used computational fluid dynamics to study the thermal transport in artificially ciliated microfluidic systems. Ciliary flow with heat transfer has many applications in bioengineering, medical sciences, and medical equipment, such as cilia-based micro devices for the clearance of viscoelastic fluid from dust and viruses.

Recently, Shaheen et al. [26] discussed the effect of nanoparticles on ciliary flow of Jeffrey fluid and resulting partial differential equations are solved by Homotopy perturbation method and Farah et al. [27] studied the electro-osmotic flow of Jeffrey fluid with effects of heat source/sink. The effect of nonlinear radiations on electro osmotic flow of viscoelastic fluid (Jeffrey fluid) due to the ciliary activity has not been considered so far to the best of our knowledge. This study serve as the first step towards understanding the role of electro-osmotically driven bio fluid flow (viscoelastic ciliary flow) with the effects of nonlinear thermal radiation and heat source which can bear the potential to bring a significant change in temperature field in the channel.

In the present work, motivated by exploring applications in thermal bio-microfluidics, a theoretical analysis of electro-osmotic bionic Jeffrey's viscoelastic flow and thermal convection in a two-dimensional channel with ciliated walls is presented. The equations of motions are formulated to include, buoyancy force, viscous dissipation [28, 29], nonlinear radiation [30, 31] and heat source [32] effects, which give the coupled system of highly nonlinear partial differential equations. To solve the resulting nonlinear coupled system, lubrication approximations and semi-analytical Homotopy perturbation method [33-35] is used. Mathematica software is employed to evaluate solutions for velocity, pressure, stream function and temperature. The effects of emerging parameters i.e. cilia length (ε), Grashof number(Gr), Brinkman number (Br), Jeffreys first viscoelastic parameter (λ_1), radiation parameter (Rn) and electroosmotic parameter (Uhs) on analytical results are visualized graphically.

2 Mathematical Modelling

Jeffrey's viscoelastic fluid flow in two-dimensional channel with ciliated walls is considered. Electroosmotic and heat transfer effects are present. An axial electrical field is imposed. The

collective beating of cilia that are present in the inner walls of the channel and buoyancy forces **[36]** produce a metachronal symplectic wave in the axial direction having constant speed c and wave lengthλ. The physical model for the problem in Cartesian coordinate system is shown in **Fig. 1**. The continuity, momentum and energy conservation equations of a bionic Jeffrey fluid with buoyancy force and potential function in the wave frame are presented as follows:
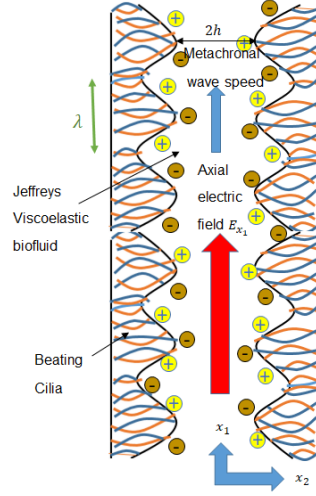

Fig. 1: Physical model for electro-osmotic flow in a ciliated channel.

$$\frac{\partial v_1}{\partial x_1} + \frac{\partial v_2}{\partial x_2} = 0, \tag{1}$$

$$\rho\left(\frac{\partial}{\partial t} + v_1\frac{\partial}{\partial x_1} + v_2\frac{\partial}{\partial x_2}\right)v_1 = -\frac{\partial p}{\partial x_1} + \frac{\partial \tau_{x_1x_1}}{\partial x_1} + \frac{\partial \tau_{x_1x_2}}{\partial x_2} \tag{2}$$
$$+\rho_e E_{x_1} + \rho g \beta_T (T - T_0),$$

$$\rho\left(\frac{\partial}{\partial t} + v_1\frac{\partial}{\partial x_1} + v_2\frac{\partial}{\partial x_2}\right)v_2 = \frac{\partial p}{\partial x_2} + \frac{\partial \tau_{x_1x_1}}{\partial x_1} + \frac{\partial \tau_{x_1x_2}}{\partial x_2}, \tag{3}$$

$$\rho c_p\left(v_1\frac{\partial}{\partial x_1} + v_2\frac{\partial}{\partial x_2}\right)T = m\left(\frac{\partial^2 T}{\partial x_1^2} + \frac{\partial^2 T}{\partial x_2^2}\right) + \tau_{x_1x_1}\left(\frac{\partial v_1}{\partial x_1}\right) \tag{4}$$

$$+\tau_{x_1x_2}\left(\frac{\partial v_1}{\partial x_2} + \frac{\partial v_2}{\partial x_1}\right) + \tau_{x_2x_2}\left(\frac{\partial v_2}{\partial x_2}\right)$$

$$-\frac{\partial q}{\partial x_2} + Q_0(T - T_0)$$

Where

$$q = \frac{16T^3\sigma^*}{3k^*}\frac{\partial T}{\partial x_2} \tag{5}$$

The stress tensor of bionic Jeffrey fluid **[21]** satisfy the following relation

$$\tau = \frac{\mu}{1+\lambda_1}\left(A_1 + \lambda_2 \frac{DA_1}{Dt}\right),$$ (6)

$$A_1 = L + L^T, L = gradV,$$ (7)

$$V = (v_1(x_1, x_2, t), v_2(x_1, x_2, t), 0).$$

The bionic viscoelastic flows are observed to be Poiseuille type which requires that flow is maximum at the center line of the ciliated channel and temperature profile is also maximum at center of channel therefore axial velocity and temperature profile at $r = 0$ (center line) satisfies the following conditions [26-27]

$$\frac{\partial v_1}{\partial x_2} = 0, v_2 = 0, \frac{\partial T}{\partial x_2} = 0 \quad at \ x_2 = 0,$$ (8a)

$$v_1 = c + \frac{-\left(\frac{2\pi}{\lambda}\right)\varepsilon\alpha ac \cos\left(\frac{2\pi}{\lambda}x_1\right)}{1 - \frac{2\pi}{\lambda}\varepsilon\alpha a \cos\left(\frac{2\pi}{\lambda}x_1\right)}, v_2 = \frac{\left(\frac{2\pi}{\lambda}\right)\varepsilon\alpha ac \sin\left(\frac{2\pi}{\lambda}x_1\right)}{1 - \frac{2\pi}{\lambda}\varepsilon\alpha a \cos\left(\frac{2\pi}{\lambda}x_1\right)}, T = T_0 \ at \ x_2 = h$$ (8b)

Where $h = a + \varepsilon\alpha \cos\left(\frac{2\pi}{\lambda}x_1\right)$

2.1 Electro hydrodynamics and potential distribution

The electric charge density ρ_e in micro channel satisfy the following Poisson equation [6]

$$\nabla^2 \Omega = -\frac{\rho_e}{\upsilon},$$ (9)

Here υ is dielectric permittivity and Ω is the electric potential function.

Also electric charge density follows the Boltzmann distribution [8] by the following relation

$$\rho_e = -2n_0 et_0 \sinh\left(\frac{et_0}{\upsilon k_b T_a}\right),$$ (10)

Applying Debye-Hückel linearization [8], Eq. (9) reduces to the following equation

$$\frac{d^2\Omega}{dx_2^2} = k\Omega,$$ (11)

Where $k = et_0\sqrt{\frac{2n_0}{\upsilon k_b T_a}}$, n_0 is the density, t_0 is elementary charge valance, e is protonic charge, k_b is the Boltzmann constant and T_a is absolute temperature.

The exact solution of Eq. (11) subject to the boundary conditions $\frac{\partial\Omega}{\partial x_2} = 0$ at $x_2 = 0$ and $\Omega = 1$ at $x_2 = h$ is as follow

$$\Omega = \frac{\cosh(kx_2)}{\cosh(kh)}.$$ (12)

2.2 Lubrication approach and non-dimensionalization

The wave frame and fixed frame are related by the following transformation

$$X_1 = x_1 - ct, \qquad X_2 = x_2, V_1 = v_1 - c, V_2 = v_2, P(X_1, X_2, t) = p(x_1, x_2, t), \tag{13}$$

where x_1, x_2, v_1, v_2 and p are the quantities in wave frame and X_1, X_2, V_1, V_2 and P are quantities in fixed frame.

The non-dimensional parameters are defined as follow

$$x_1^* = \frac{x_1}{a}, x_2^* = \frac{x_2}{\lambda}, v_2^* = \frac{v_2}{c}, v_1^* = \frac{v_1}{\beta c}, h^* = \frac{H}{a}, \Omega^* = \frac{\Omega}{\xi}, \beta = \frac{a}{\lambda}, p^* = \frac{a^2 p}{c\mu\lambda}, \tau_{ij}^* = \frac{a}{\mu c} \tau_{ij}, \tag{14}$$

$$Re = \frac{\rho\beta ac}{\mu}, Uhs = \frac{E_r \eta \xi}{\mu c}, Gr = \frac{g\beta a^3}{\nu}(T_1 - T_0), Pr = \frac{\mu c_p}{m}, Ec = \frac{c^2}{(T_1 - T_0)}, Br = Pr.Ec$$

$$\eta^2 = \frac{Q_0 a^2}{mc_p\mu}, \theta = \frac{T - T_0}{T_0 - T_1}, \theta_w = \frac{T_1}{T_0}, Rn = \frac{16T_0^3\sigma^*}{3mk^*}.$$

All parameter definitions are given in the notation section. In view of Eq. (14), after applying the lubrication approach and ignoring the inertial forces [**34**] and dropping asterisks Eq. (2)-(4) and (7) then take the following form:

$$\frac{\partial p}{\partial x_1} = \frac{1}{1+\lambda_1} \frac{\partial}{\partial x_2}\left(1 + \lambda_2\beta\left(u\frac{\partial}{\partial x_1} + v\frac{\partial}{\partial x_2}\right)\right)\frac{\partial v_1}{\partial x_2} - k^2 Uhs\Omega + Gr\theta, \tag{15}$$

$$\frac{\partial p}{\partial x_2} = 0, \tag{16}$$

$$\frac{\partial^2\theta}{\partial x_2^2} + \eta\theta = \frac{-Br}{1+\lambda_1}\left(1 + \lambda_2\beta\left(u\frac{\partial}{\partial x_1} + v\frac{\partial}{\partial x_2}\right)\right)\left(\frac{\partial v_1}{\partial x_2}\right)^2$$

$$-Rn(1 + (\theta_w - 1)\theta)^3 \frac{\partial^2\theta}{\partial x_2^2}. \tag{17}$$

The centre line symmetry assumption and metachronal wave at the tip of the cilia gives the following dimensionless boundary conditions

$$v_1 = -1 - 2\pi\varepsilon\alpha\beta \cos(2\pi x_1), \tag{18a}$$

$$v_2 = 2\pi\varepsilon \sin(2\pi x_1) + (2\pi\varepsilon)^2\alpha\beta \sin(2\pi x_1) \cos(2\pi x_1) \tag{18b}$$

$$\theta = 0, \ at \ x_2 = h = 1 + \varepsilon \cos(2\pi x_1) \tag{18c}$$

$$\frac{\partial v_1}{\partial x_2} = 0, \ v_2 = 0, \qquad \frac{\partial\theta}{\partial x_2} = 0 \ at \ x_2 = 0 \tag{18d}$$

The stream function ψ is defined as

$$v_1 = \frac{\partial\psi}{\partial x_2}, \ v_2 = -\frac{\partial\psi}{\partial x_1}. \tag{19}$$

Eqs. (15)-(18) in terms of ψ take the following form

$$\frac{\partial^4 \psi}{\partial y^4} = (1 + \lambda_1)\left(k^2 Uhs\frac{\partial\Omega}{\partial x_2} - Gr\frac{\partial\theta}{\partial x_2}\right) + \lambda_2\beta\frac{\partial^2}{\partial x_2{}^2}\left(\frac{\partial\psi}{\partial x_2}\frac{\partial}{\partial x_1} - \frac{\partial\psi}{\partial x_1}\frac{\partial}{\partial x_2}\right)\frac{\partial^2\psi}{\partial x_2{}^2} \tag{20}$$

$$\frac{\partial^2\theta}{\partial x_2^2} + \eta\theta = \frac{-Br}{1 + \lambda_1}\left(1 + \lambda_2\beta\left(u\frac{\partial}{\partial x_1} + v\frac{\partial}{\partial x_2}\right)\right)\left(\frac{\partial v_1}{\partial x_2}\right)^2 - Rn(1 + (\theta_w - 1)\theta)^3\frac{\partial^2\theta}{\partial x_2^2} \tag{21}$$

The boundary conditions can be expressed as

$$\psi = 0, \quad \frac{\partial^2\psi}{\partial x_2{}^2} = 0, \quad \frac{\partial\theta}{\partial x_2} = 0, \quad at \ \ x_2 = 0, \tag{22a}$$

$$\psi = F, \quad \frac{\partial\psi}{\partial x_2} = -1 - 2\pi\varepsilon\alpha\beta\cos(2\pi x_1), \quad \theta = 0, \tag{22b}$$

$$\frac{\partial\psi}{\partial x_1} = 2\pi\varepsilon\sin(2\pi x_1) + \beta(2\pi\varepsilon)^2\alpha\sin(2\pi x_1)\cos(2\pi x_1), \quad at \ x_2 = h.$$

3 HPM Solution Methodology

To solve this system of coupled nonlinear partial differential equations, the Homotopy perturbation method (HPM) is used. This method was developed by He [**33**] and has been applied to numerous viscoelastic biological propulsion problems [**34, 35**]. The Homotopic structure for velocity and temperature fields are defined as follows:

$$H_1(\psi, q) = (1 - q)\left(L_1(\psi) - L_1(\widetilde{\psi_0})\right) + q\left(L_1(\psi) + N_1(\psi) + g_\psi(x_2) = 0\right), \tag{23a}$$

$$H_1(\theta, q) = (1 - q)\left(L_2(\theta) - L_2(\tilde\theta_0)\right) + q\left(L_2(\theta) + N_2(\theta) + g_\theta(x_2) = 0\right), \tag{23b}$$

Here L_1 and L_2 are linear operators, g_ψ and g_θ are known functions, $\tilde v_0$ and $\tilde\theta_0$ are initial approximations and chosen as follows:

$$L_1 = \frac{\partial^4}{\partial x_2^4}, \qquad L_2 = \frac{\partial^2}{\partial x_2^2}, \tag{24a}$$

$$\widetilde{\psi_0} = \left(\frac{3F_0 - hu(h)}{2h}\right)x_2 - \left(\frac{F_0 - hu(h)}{2h^3}\right)x_2{}^3, \qquad \tilde\theta_0 = \frac{(x_2^2 - h^2)}{4}, \tag{24b}$$

$$N(\psi) = \beta\lambda_2\left(-\frac{\partial\psi}{\partial x_1}\frac{\partial^5\psi}{\partial x_2{}^5} + \frac{\partial\psi}{\partial x_2}\frac{\partial^5\psi}{\partial x_1\partial x_2{}^4} + 2\frac{\partial^2\psi}{\partial x_2{}^2}\frac{\partial^4\psi}{\partial x_1\partial x_2{}^3} - 2\frac{\partial^4\psi}{\partial x_2{}^4}\frac{\partial^2\psi}{\partial x_1\partial x_2}\right), \tag{24c}$$

$$N(\theta) = -\frac{Br}{(1+\lambda_1)}\left(\left(\frac{\partial^2\psi}{\partial x_2{}^2}\right)^2 + \beta\lambda_2\left(\frac{\partial^2\psi}{\partial x_2{}^2}\frac{\partial\psi}{\partial x_2} + \frac{\partial^3\psi}{\partial x_1\partial x_2{}^2} - \frac{\partial\psi}{\partial x_1}\frac{\partial^3\psi}{\partial x_2{}^3}\right)\right) \tag{24d}$$

$$- Rn(1 + (\theta_w - 1)\theta)^3\frac{\partial^2\theta}{\partial x_2^2},$$

$$g_\psi(x_2) = (1+\lambda_1)(k^2Uhs\Omega - Gr\theta), \quad g_\theta(x_2) = -\eta\theta_0. \tag{24e}$$

The solutions of Eq. (23) can be obtained as power series expansions:

$$\psi = \psi_0 + q\psi_1 + q^2\psi_2 + q^3\psi_{3+\cdots} \tag{25a}$$

$$\theta = \theta_0 + q\theta_1 + q^2\theta_2 + q^3\theta_{3+\cdots} \tag{25b}$$
$$F = F_0 + qF_1 + q^2F_2 + q^3F_{3+\cdots} \tag{25c}$$

Here $q \in [0,1]$ is an embedding parameter with values 0 and 1 gives the initial and final solution. Using Eq. (25a-25c) in Eq. (20) and (21) one can determine the zero, first and second order systems which are given in appendix and solutions for first, second and third order system are calculated with the help of software "MATHEMATICA".

To find Q, volumetric flow rate, and related to the flux by the following relation

$$Q = \int_0^h\left(\frac{\partial\psi}{\partial y} + 1\right)dy = F + h. \tag{26}$$

Furthermore, the axial pressure gradient in terms of velocity and temperature profile is computed as:

$$\frac{\partial p}{\partial x_1} = \frac{1}{1+\lambda_1}\frac{\partial}{\partial x_2}\left(1 + \lambda_2\beta\left(u\frac{\partial}{\partial x_1} + v\frac{\partial}{\partial x_2}\right)\right)\frac{\partial v_1}{\partial x_2} - k^2Uhs\Omega + Gr\theta. \tag{27}$$

The solution obtained by the Homotopy perturbation method are calculated for pressure gradient, velocity and temperature in the form of power series with decaying coefficients.

4 Results and Discussion

To plot graphical results based on the solutions developed in section 4, Mathematica software is employed. All computations are visualized in **Figs. 2-7**. The default values used in the simulations are prescribed as follows: $\alpha = 0.2$, $\beta = 0.2$, $x_1 = 0.25$, $k = 0.2$ and $\varepsilon = 0.3$, these are consistent with standard works in the area of ciliated propulsion. **Fig. 2$(a - d)$** portrays the effects of Grashof number (Gr), Jeffrey fluid parameter (λ_1, λ_2) and Helmholtz-Smoluchowski velocity (Uhs) on axial velocity. It is observed that magnitude of axial velocity decreases with increasing Jeffrey fluid parameter (λ_1) and increases with increasing Grashof number (Gr),

Jeffrey fluid parameter (λ_2) and Helmholtz-Smoluchowski velocity (Uhs). The thermal buoyancy force, $Gr\theta$ in the momentum equation has a significant impact on flow development. $G_r = \frac{g\beta a^3}{\nu}(T_1 - T_0)$ represents the ratio of thermal buoyancy force to viscous force. For $Gr < 1$, the viscous force exceeds the thermal buoyancy force, and this is the range considered in **Fig. 2a**. Axial flow acceleration is clearly induced with increase in Grashof number. Similarly, higher values of the viscoelastic parameter (ratio of relaxation to retardation times i.e. λ_1) decrease the axial flow, which support the findings of Lu *et al.* [14] confirming that viscoelastic media achieve decreased flow performance. By increasing Jeffrey fluid parameter (λ_2) fluid's velocity increases shown in **Fig. 2c**. With higher values of *Uhs*, axial electrical field, E_{x_1}, is stronger ($Uhs = \frac{E_{x_1}\nu}{\mu c}$), and this also enhances the axial flow in accordance with the term, $Uhs\Omega$ in the momentum that is shown in **Fig. 2d**. The acceleration is sustained across the span of the micro channel and a Poiseuille-type distribution is generated (velocity peak at the channel centre line).

Fig. 3(a-b) illustrate the impact of cilia length parameter (ε) and Jeffrey fluid parameters (λ_1, λ_2) on pressure gradient. It is noticed that pressure gradient increases along the axial direction of the channel as we increase cilia length parameter (ε) and Jeffrey fluid parameter (λ_2) and a decrease can be observed with the increasing value of Jeffrey fluid parameter (λ_1). The peripheral regions of the channel do not exhibit any significant modifications in pressure gradient, which are confined to the core zone. However, increasing viscoelastic effect is known to accelerate the flow which induces the opposite effect in pressure gradient. These trends concur with earlier studies on viscoelastic thermal electro-osmotic flows.

Fig. 4(a-f) portrays the variation of temperature field for distinct values of Grashof number (Gr), Brinkman number (Br), Jeffrey fluid parameters (λ_1, λ_2), nonlinear radiation (Rn) and Helmholtz-Smoluchowski velocity (Uhs). It is observed that with an increment in Jeffrey fluid parameter (λ_1) and Helmholtz-Smoluchowski velocity(Uhs) there is a significant elevation in temperatures. Stronger thermal buoyancy (Gr) as shown in **Fig.4a**, significantly suppresses temperatures, which is a characteristic feature of buoyancy-driven flows, as noted by Gebhart *et al*. [**36**]. With increasing Brinkman number, B_r and *Rn* through **Fig. 4b, Fig. 4f** a strong reduction in temperatures is also observed. Brinkman number quantifies the ratio of heat generated by viscous dissipation and the propagation of heat by molecular conduction in the fluid. When $Br = 1$ both dissipation and molecular conduction are equivalent. However, for $Br > 1$, dissipation

exceeds conduction and this manifests in an elevation in temperatures. With greater viscoelasticity (**Fig. 4c**), the upsurge in viscosity is conducive to thermal diffusion which results in heating of the regime. Increasing the values of Jeffrey fluid parameter (λ_2) temperature profile decreases. Higher values of Helmholtz-Smoluchowski velocity also correspond to stronger axial electrical field which again contributes to enhanced heating of the bionic fluid (**Fig. 4d**) i.e. elevation in temperatures.

Fig. 5(a-c) indicate that with increasing Grashof number Gr, there is a general reduction in bolus sizes in the channel, although again the number of boluses is unaffected. In particular, there is a greater constriction of boluses in the axial direction with an elongation induced in the transverse direction. The clustering of streamlines at the upper and lower peripheries is therefore also intensified with greater thermal buoyancy effect. In **Fig. 6a-c**, increasing Helmholtz-Smoluchowski velocity (Uhs) i.e. stronger axial electrical field induces a considerable expansion in bolus structure and growth in both directions, also leading to the emergence of smaller-scale boluses at Uhs =3. Clearly the bionic flow exhibits considerable sensitivity to electrical field effects and provides a useful mechanism for controlling such flows in bio-microfluidics. Finally, In **Fig. 7(a-c)**, it is noted that the nonlinear radiation leading to reduction in number of boluses and their size, because the nonlinear radiation in the EOF causes to increase the resistance in the fluid flow and the molecular forces between the fluid particles become strong.
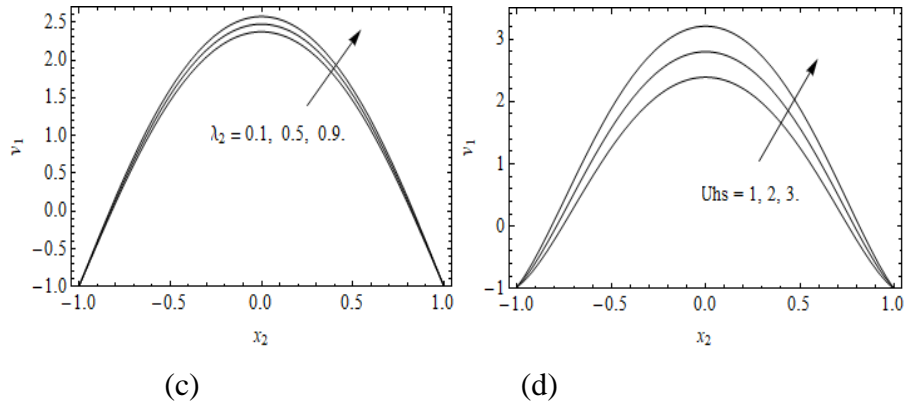

(a)   (b)
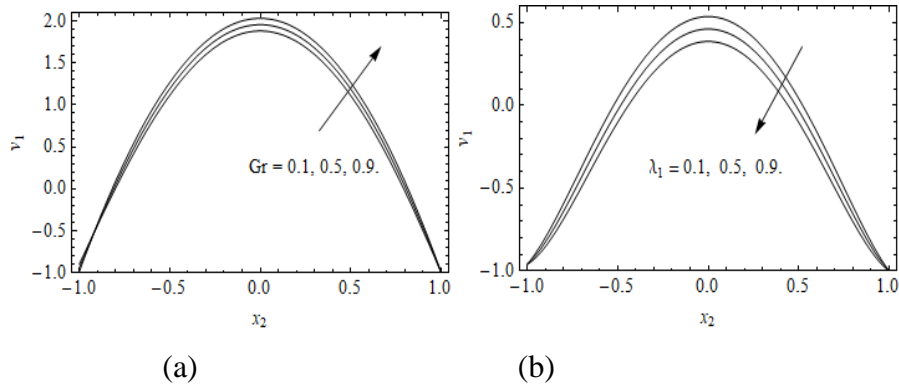
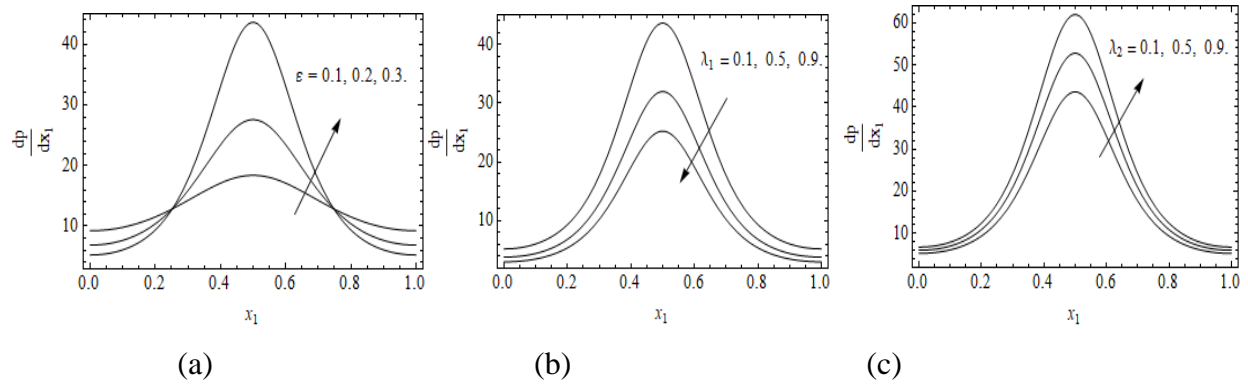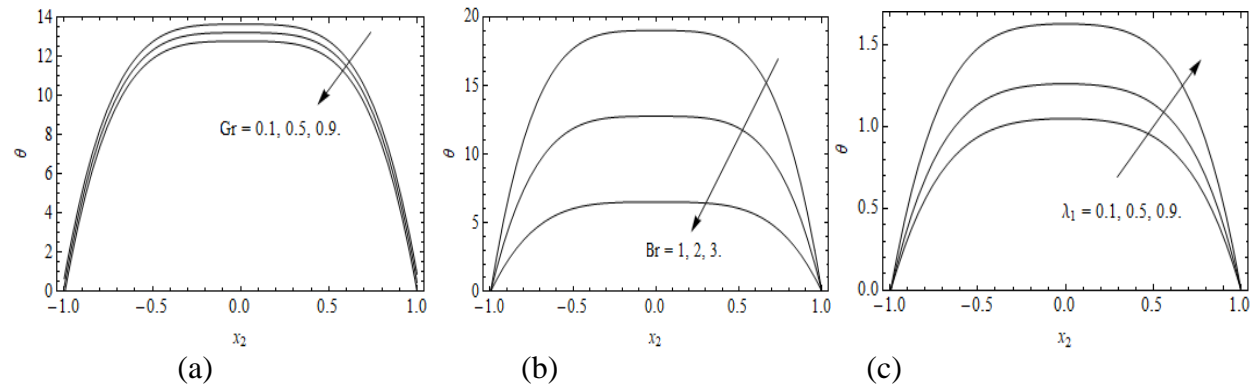**Fig. 2a-d**: Variation of axial velocity for increasing values of Gr, λ_1, λ_2 and Uhs.

Fig. 3a- c: Variation of pressure gradient, $\dfrac{dp}{dx_1}$ for increasing values of ε, λ_1 and λ_2.

(d)   (e)   (f)
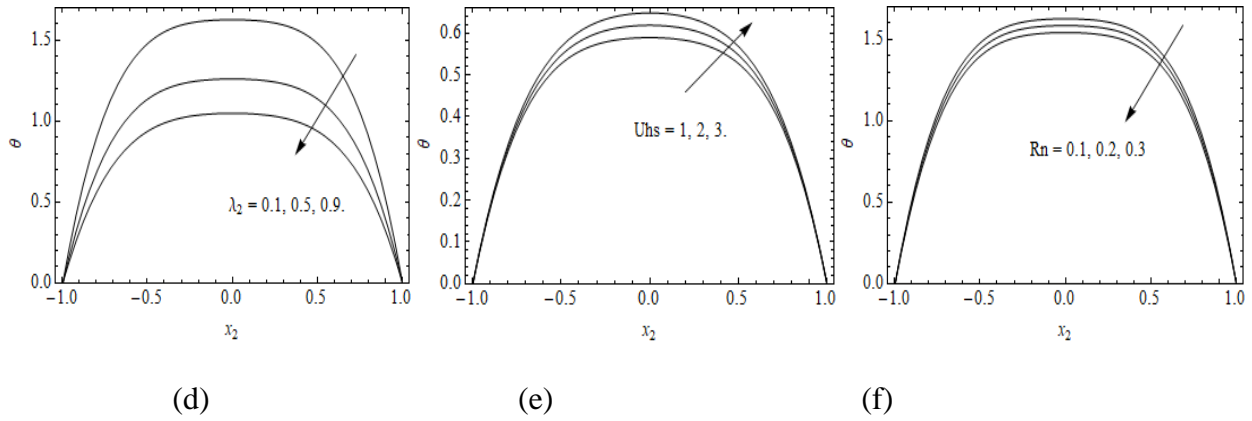
Fig. 4a-f: Temperature distributions θ for increasing values of $Gr,\ Br,\ \lambda_1,\ \lambda_2, Uhs$ and Rn.

(a) $Gr = 0.1$ (b) $Gr = 0.5$ (c) $Gr = 0.9$
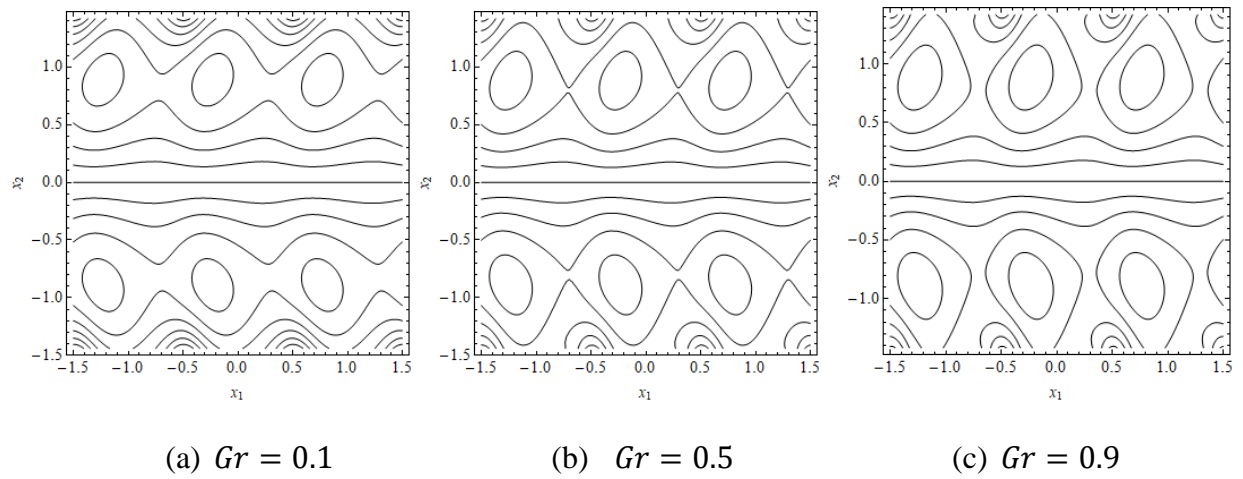
Fig. 5a-c: Streamline distributions ψ for increasing values of Gr.

(a) $Uhs = 1$ (b) $Uhs = 2$ (c) $Uhs = 3$
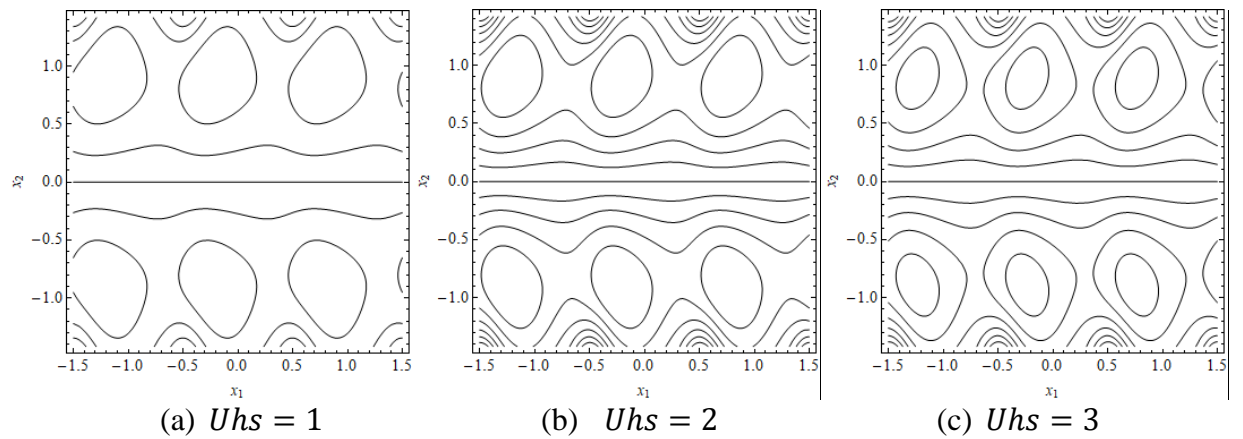
Fig. 6a-c: Streamline distributions ψ for increasing values of Uhs.

(a) $Rn = 0.1$ (b) $Rn = 0.2$ (c) $Rn = 0.3$

Fig. 7a-c: Streamline distributions ψ for increasing values of Rn.

5 Conclusions

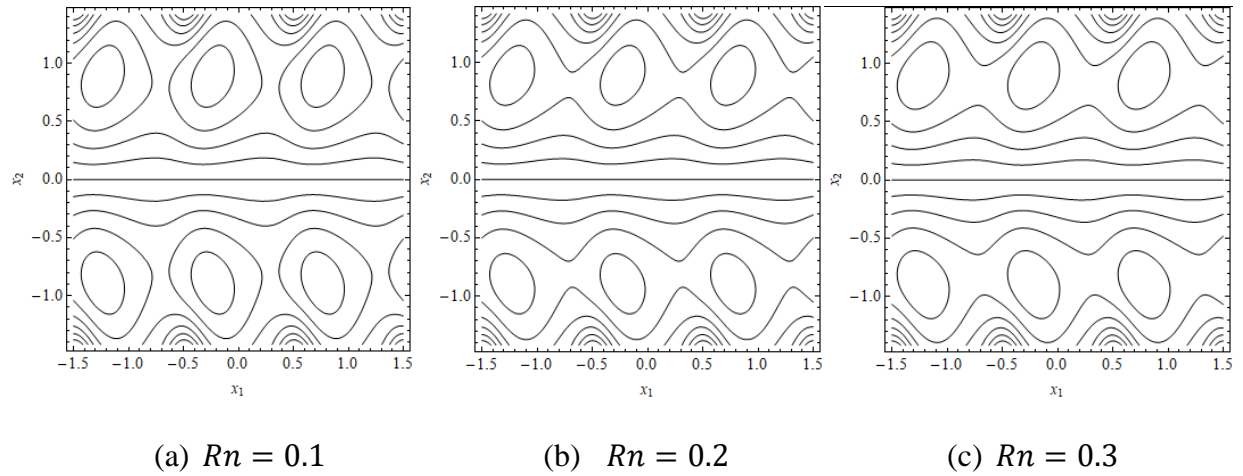A mathematical analysis of electroosmotic mixed convective bionic viscoelastic flow generated by metachronal beating of cilia in a channel with heat generation and viscous dissipation effects under static axial electrical field, has been presented. **Mathematica** symbolic software is employed to evaluate numerically and graphically visualize the influence of key thermophysical, geometric and electro-osmotic parameters on transport characteristics. Axial flow is observed to slow down with larger thermal buoyancy forces (increasing Grashof number), positive values of Helmholtz-Smoluchowski (electro-osmotic) velocity (reversed axial electrical field) and Jeffrey fluid viscoelastic relaxation parameter. The simulations have shown that: Axial flow velocity is reduced increasing Grashof number, Jeffreys viscoelastic fluid parameter and Helmholtz-Smoluchowski velocity.

- Axial Pressure gradient is increased with an increase in cilia length parameter whereas it is suppressed with greater values of Jeffrey fluid parameter.

- Temperature magnitudes are enhanced with Jeffrey fluid parameter, Brinkman number and Helmholtz-Smoluchowski velocity whereas they are reduced with thermal buoyancy effect i.e. greater values of Grashof number.

- Bolus (trapped circulation zone) size is enhanced with increasing values of, Grashof number, heat generation parameter and Helmholtz-Smoluchowski velocity whereas it diminishes with higher values of radiation parameter.

- We believe that this analysis, besides providing a deep theoretical insight to interpret the transport process, will also serve as a fundamental design tool for microfluidic devices/systems under electro kinetic influence.
- In the present study we have considered ciliary flow as a single layer; future studies may examine ciliary flow in two layers i.e. liquid-liquid and liquid-solid phases.

Nomenclature

Symbols	Meaning	Symbols	Meaning
		Greek letters	
X_1, X_2	Axial and transverse coordinates in fixed frame	α	Eccentricity of ellipse
x_1, x_2	Axial and transverse coordinates in wave frame	Ω	Electrical potential function
V_1, V_2	Axial and transverse velocity in fixed frame		
v_1, v_2	Axial and transverse velocity in wave frame	λ_1, λ_2	Jeffrey viscoelastic parameters
t_0	Elementary charge valence	ϵ	Cilia length
Gr	Grashof number	τ	Cauchy stress
$\boldsymbol{g}$	Acceleration due to gravity	ρ_e	Electric charge density
k	Electroosmotic parameter	ψ	Stream function
Br	Brinkman number	β	Wave number
Uhs	Helmholtz-Smoluchowski velocity	λ	Wavelength
c	Metachronal wave speed	ρ	Density of the fluid
n_0	Number density	μ	Dynamic viscosity of fluid
P	Pressure distribution in fixed frame	β_T	Thermal expansion coefficient
p	Pressure distribution in wave frame	υ	Dielectric permittivity of the medium
Q_0	Heat source/sink	σ^*	Stefan--Boltzmann coefficient
E_{x_1}	Applied electric field	k^*	Rosseland mean absorption coefficient
Pr	Prandtl number		
Ec	Eckert number		
c_p	Specific heat		
e	Protonic charge		
m	Thermal conductivity of the bionic fluid		
T	Temperature field		
k_b	Boltzmann constant		
T_a	Absolute temperature		
T_0	Temperature at the centre of the channel		
T_1	Temperature on the ciliated surface		

Rn Radiation parameter

Appendix
Zeroth order system

$$\frac{\partial^4 \psi_0}{\partial x_2^2} - \frac{\partial^4 \tilde{\psi}_0}{\partial x_2^4} = 0,$$

$$\frac{\partial^2 \theta_0}{\partial x_2^2} - \frac{\partial^2 \tilde{\theta}_0}{\partial x_2^2} = 0,$$

The associated boundary conditions

$$\psi_0 = 0, \quad \frac{\partial^2 \psi_0}{\partial x_2{}^2} = 0, \quad \frac{\partial \theta_0}{\partial x_2} = 0, \quad at \quad x_2 = 0,$$

$$\psi_0 = F, \quad \frac{\partial \psi_0}{\partial x_2} = -1 - 2\pi\varepsilon\alpha\beta \cos(2\pi x_1), \quad \theta_0 = 0, \quad at \; x_2 = h.$$

First order system

$$\frac{\partial^4 \psi_1}{\partial y^4} = -\frac{\partial^4 \psi_0}{\partial y^4} + (1 + \lambda_1)\left(k^2 Uhs \frac{\partial \Omega}{\partial x_2} - Gr \frac{\partial \theta_0}{\partial x_2}\right)$$

$$+\beta\lambda_2\left(-\frac{\partial \psi_0}{\partial x_1}\frac{\partial^5 \psi_0}{\partial x_2{}^5} + \frac{\partial \psi_0}{\partial x_2}\frac{\partial^5 \psi_0}{\partial x_1 \partial x_2{}^4} + 2\frac{\partial^2 \psi_0}{\partial x_2{}^2}\frac{\partial^4 \psi_0}{\partial x_1 \partial x_2{}^3} - 2\frac{\partial^4 \psi_0}{\partial x_2{}^4}\frac{\partial^2 \psi_0}{\partial x_1 \partial x_2}\right)$$

$$\frac{\partial^2 \theta_1}{\partial x_2^2} = -\frac{\partial^2 \theta_0}{\partial x_2^2} - \eta\theta_0 - Rn(1 + (\theta_w - 1)\theta_0)^3 \frac{\partial^2 \theta_0}{\partial x_2^2}$$

$$-\frac{Br}{(1+\lambda_1)}\left(\left(\frac{\partial^2 \psi_0}{\partial x_2{}^2}\right)^2 + \beta\lambda_2\left(\frac{\partial^2 \psi_0}{\partial x_2{}^2}\frac{\partial \psi_0}{\partial x_2} + \frac{\partial^3 \psi_0}{\partial x_1 \partial x_2{}^2} - \frac{\partial \psi_0}{\partial x_1}\frac{\partial^3 \psi_0}{\partial x_2{}^3}\right)\right)$$

and the associated boundary conditions are

$$\psi_1 = 0, \quad \frac{\partial^2 \psi_1}{\partial x_2{}^2} = 0, \quad \frac{\partial \theta_1}{\partial x_2} = 0, \quad at \quad x_2 = 0,$$

$$\psi_1 = 0, \quad \frac{\partial \psi_1}{\partial x_2} = 0, \quad \theta_1 = 0, \quad at \; x_2 = h.$$

Second order system

$$\frac{\partial^4 \psi_2}{\partial y^4} = -(1 + \lambda_1)\left(Gr \frac{\partial \theta_1}{\partial x_2}\right)$$

$$+\beta\lambda_2\left(\begin{array}{c}-\dfrac{\partial \psi_0}{\partial x_1}\dfrac{\partial^5 \psi_1}{\partial x_2{}^5} - \dfrac{\partial \psi_1}{\partial x_1}\dfrac{\partial^5 \psi_0}{\partial x_2{}^5} + \dfrac{\partial \psi_0}{\partial x_2}\dfrac{\partial^5 \psi_1}{\partial x_1 \partial x_2{}^4} + \dfrac{\partial \psi_1}{\partial x_2}\dfrac{\partial^5 \psi_0}{\partial x_1 \partial x_2{}^4} \\[2mm] +2\dfrac{\partial^2 \psi_0}{\partial x_2{}^2}\dfrac{\partial^4 \psi_1}{\partial x_1 \partial x_2{}^3} + 2\dfrac{\partial^2 \psi_1}{\partial x_2{}^2}\dfrac{\partial^4 \psi_0}{\partial x_1 \partial x_2{}^3} - 2\dfrac{\partial^4 \psi_0}{\partial x_2{}^4}\dfrac{\partial^2 \psi_1}{\partial x_1 \partial x_2} - 2\dfrac{\partial^4 \psi_1}{\partial x_2{}^4}\dfrac{\partial^2 \psi_0}{\partial x_1 \partial x_2}\end{array}\right),$$

$$\frac{\partial^2 \theta_2}{\partial x_2^2} = -\eta \theta_1 - \frac{Br}{(1+\lambda_1)}\left(\frac{\partial^2 \psi_0}{\partial x_2{}^2}\frac{\partial \psi_1}{\partial x_2} + \frac{\partial^2 \psi_1}{\partial x_2{}^2}\frac{\partial \psi_0}{\partial x_2} + \frac{\partial^3 \psi_1}{\partial x_1 \partial x_2{}^2} - \frac{\partial \psi_0}{\partial x_1}\frac{\partial^3 \psi_1}{\partial x_2{}^3} - \frac{\partial \psi_1}{\partial x_1}\frac{\partial^3 \psi_0}{\partial x_2{}^3}\right)$$

$$- \frac{2Br}{(1+\lambda_1)}\frac{\partial^2 \psi_0}{\partial x_2{}^2}\frac{\partial^2 \psi_1}{\partial x_2{}^2} - 3Rn\big((\theta_w - 1)\theta_1\big)\frac{\partial^2 \theta_0}{\partial x_2^2} + 6Rn(\theta_w - 1)^2\theta_0\theta_1\frac{\partial^2 \theta_0}{\partial x_2^2}$$

$$+ 3Rn\big((\theta_w - 1)\theta_1\theta_0^2\big)\frac{\partial^2 \theta_0}{\partial x_2^2} + Rn(\theta_w - 1)\theta_0^3\frac{\partial^2 \theta_1}{\partial x_2^2} + Rn\frac{\partial^2 \theta_1}{\partial x_2^2}$$

$$+ 3Rn\big((\theta_w - 1)\theta_0\big)\frac{\partial^2 \theta_1}{\partial x_2^2} + 3Rn\big((\theta_w - 1)\theta_0^2\big)\frac{\partial^2 \theta_1}{\partial x_2^2} = 0.$$

and the associated boundary conditions are

$$\psi_2 = 0, \quad \frac{\partial^2 \psi_2}{\partial x_2{}^2} = 0, \quad \frac{\partial \theta_2}{\partial x_2} = 0, \quad at \quad x_2 = 0,$$

$$\psi_2 = 0, \quad \frac{\partial \psi_2}{\partial x_2} = 0, \quad \theta_2 = 0, \quad at \quad x_2 = h.$$

References

[1] Li, Dongqing, ed. Encyclopedia of microfluidics and nanofluidics. *Springer Science & Business edia*, 2008.

[2] Yoo, K, Shim, J, & Dutta, P. Effect of Joule heating on isoelectric focusing of proteins in a microchannel. *Biomicrofluidics*, 2014, **8**.

[3] Green N G, Ramos A, organ H. Numerical solution of the dielectrophoretic and travelling wave forces for interdigitated electrode arrays using the finite element method. Journal of *Electrostatisttics*, 2002, **56(2)**, 235-254.

[4] Mauck R L, Hung C T, Ateshian G A. Modeling of neutral solute transport in a dynamically loaded porous permeable gel: implications for articular cartilage biosynthesis and tissue engineering. *Journal of Biomechanical Engineering*, 2014, **125(5)**, 602-614.

[5] Yongbin WANG, Junhong GUO. Effective electroelastic constants for three-phase confocal elliptical cylinder model in piezoelectric quasicrystal composites [J]. Applied Mathematics and Mechanics (English Edition), 2018, **39(6)**, 797-812.

[6] Yongbo LIU, Yongjun JIAN. Electroviscous effect on electromagnetohydrodynamic flows of Maxwell fluids in parallel plate microchannels [J]. Applied Mathematics and Mechanics (English Edition), 2019, **40(10)**, 1457-1470.

[7] Ooi K T, Yang C, Chai J C, Wong T N. Developing electro-osmotic flow in closed-end micro-channels. *International Journal of Engineering Science*, 2005, **43(17-18)**, 1349-1362.

[8] Tripathi D, Bhushan S, Bég O A. Analytical study of electro-osmosis modulated capillary peristaltic hemodynamics. *Journal of Mechanics in Medicine and Biology*, 2017, **17(03)**, 1750052.

[9]   Ng C O. Combined pressure-driven and electroosmotic flow of Casson fluid through a slit microchannel. *Journal of Non-Newtonian Fluid Mechanics*, 2013, **198**, 1-9.

[10] Ali N, Hussain S, Ullah K, Bég O A. Mathematical modelling of two-fluid electro-osmotic peristaltic pumping of an Ellis fluid in an axisymmetric tube. *The European Physical Journal Plus*, 2019, **134(4)**, 141.

[11] Sánchez S, Arcos J, Bautista O, Méndez F. Joule heating effect on a purely electroosmotic flow of non-Newtonian fluids in a slit microchannel. *Journal of Non-Newtonian Fluid Mechanics*, 2013, **192**, 1-9.

[12] M. Farooq, A. Alsaedi, T. Hayat. Note on characteristics of homogeneous-heterogeneous reaction in flow of Jeffrey fluid [J]. Applied Mathematics and Mechanics (English Edition), 2015, 36(10): 1319-1328.

[13] Narla V K, Tripathi D, Bég O A. Electro-osmosis modulated viscoelastic embryo transport in uterine hydrodynamics: mathematical modeling. *Journal of biomechanical engineering*, 2019, **141(2)**.

[14] Corey D P, Hudspeth A J. Ionic basis of the receptor potential in a vertebrate hair cell. *Nature*, 1979, **281(5733)**, 675-7.

[15] Wang Z, Wu H J, Fine D, Schmulen J, Hu Y, Godin B, Zhang JX, Liu X. Ciliated micropillars for the microfluidic-based isolation of nanoscale lipid vesicles. *Lab on a Chip*, 2013, **13(15)**, 2879-82.

[16] Vasudevan M, Lange C F. Property dependence of onset of instability in viscoelastic respiratory fluids. *International journal of engineering science*, 2005, **43(15-16)**, 1292-8.

[17] den Toonder J, Bos F, Broer D, Filippini L, Gillies M, de Goede J, Mol T, Reijme M, Talen W, Wilderbeek H, Khatavkar V. Artificial cilia for active micro-fluidic mixing. *Lab on a Chip*, 2008, **8(4)**, 533-41.

[18] Balazs A C, Bhattacharya A, Tripathi A, Shum H. Designing bioinspired artificial cilia to regulate particle--surface interactions. *The journal of physical chemistry letters*, 2014, **5(10)**, 1691-700.

[19] Chateau S, Favier J, D'ortona U, Poncet S. Transport efficiency of metachronal waves in 3D cilium arrays immersed in a two-phase flow. *Journal of Fluid Mechanics*, 2017, **824**, 931-61.

[20] Manzoor N, Bég O A, Maqbool K, Shaheen S. Mathematical modelling of ciliary propulsion of an electrically-conducting Johnson-Segalman physiological fluid in a channel with slip. *Computer methods in biomechanics and biomedical engineering*, 2019, **22(7)**, 685-95.

[21] Manzoor N, Maqbool K, Bég O A, Shaheen S. Adomian decomposition solution for propulsion of dissipative magnetic Jeffrey biofluid in a ciliated channel containing a porous medium with forced convection heat transfer. *Heat Transfer-Asian Research,* 2019, **48(2)**, 556-81.

[22]   Maqbool K, Shaheen S, Mann A B. Exact solution of cilia induced flow of a Jeffrey fluid in an inclined tube. *SpringerPlus*, 2016**, 5(1)**, 1-6.

[23]   Mercke U. The influence of varying air humidity on mucociliary activity. *Acta oto-laryngologica*, 1975, **79(1-2)**, 133-9.

[24]   Prodromou N V, Thompson C L, Osborn D P, Cogger K F, Ashworth R, Knight M M, Beales P L, Chapple J P. Heat shock induces rapid resorption of primary cilia. *Journal of cell science*, 2012, **125(18)**, 4297-305.

[25]   Mills Z G, Aziz B, Alexeev A. Beating synthetic cilia enhance heat transport in microfluidic channels. *Soft Matter*, 2012, **8(45)**, 11508-13.

[26]   Shaheen S, Maqbool K, Siddiqui AM. Micro rheology of Jeffrey nanofluid through cilia beating subject to the surrounding temperature. Rheologica Acta. 2020 ;59(8):565-73.

[27]   Gul F, Maqbool K, Mann AB. Thermal analysis of electroosmotic flow in a vertical ciliated tube with viscous dissipation and heat source effects. Journal of Thermal Analysis and Calorimetry. 2020,1.

[28]   Akbar N S, Tripathi D, Bég O A, Khan Z H. MHD dissipative flow and heat transfer of Casson fluids due to metachronal wave propulsion of beating cilia with thermal and velocity slip effects under an oblique magnetic field. *Acta Astronautica*, 2016, **128**, 1-2.

[29]   Akbar N S, Khan L A, Khan Z H, Mir N A. Natural propulsion with lorentz force and nanoparticles in a bioinspired lopsided ciliated channel. *Journal of Bionic Engineering*, 2017, **14(1)**, 172-81.

[30]   Hussain Q, Latif T, Alvi N, Asghar S. Nonlinear radiative peristaltic flow of hydromagnetic fluid through porous medium. *Results in Physics*. 2018, **9**, 121-34.

[31]   Kothandapani M, Prakash J. Influence of heat source, thermal radiation, and inclined magnetic field on peristaltic flow of a hyperbolic tangent nanofluid in a tapered asymmetric channel. IEEE transactions on nanobioscience. 2014, **14(4),** 385-92.

[32]   Bég O A, Beg T A, Karim I, Khan M S, Alam M M, Ferdows M, Shamshuddin M D. Numerical study of magneto-convective heat and mass transfer from inclined surface with Soret diffusion and heat generation effects: A model for ocean magnetic energy generator fluid dynamics. *Chinese Journal of Physics*, 2019, **60**, 167-79.

[33]   He JH. Homotopy perturbation method: a new nonlinear analytical technique. *Applied Mathematics and computation*, 2003, **135(1)**, 73-9.

[34]   Tripathi D, Bég O A. A numerical study of oscillating peristaltic flow of generalized Maxwell viscoelastic fluids through a porous medium. *Transport in porous media*, 2012, **95(2)**, 337-48.

[35]   Alarabi T, Elsayed A F, Bég O A. Homotopy perturbation method for heat transfer in peristaltic flow of viscoelastic fluid in an eccentric cylinder with variable effects. *Life Science Journal*, 2014, **11(7)**, 197-206.

[36]   Gebhart B, Jaluria Y, Mahajan RL, Sammakia B. Buoyancy-induced flows and transport. 1988.